Supplementary information

The impact of ionic liquids on the coordination of anions with solvatochromic copper complexes

Olga Kuzmina[a], Nur Hasyareeda Hassan,[a, b] Laura Patel[a], Claire Ashworth,[a] Eduards Bakis,[a] Andrew J. P. White,[a] Patricia A. Hunt[a,] and Tom Welton[a,*]*

[a]Department of Chemistry, Imperial College London, London SW7 2AZ, UK
[b]School of Chemical Sciences and Food Technology, Universiti Kebangsaan Malaysia

Section 1: Synthesis of Ionic Liquids

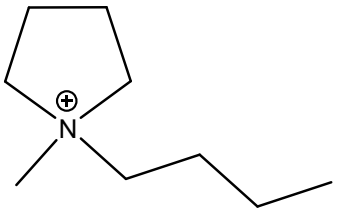

1-butyl-1-methylpyrrolidinium

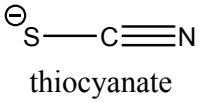

thiocyanate

chloride

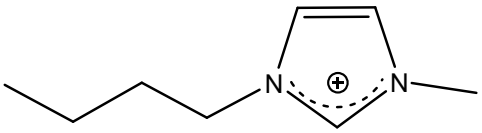

1-butyl-3-methylimidazolium

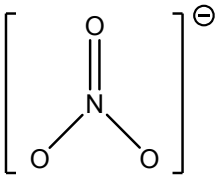

nitrate

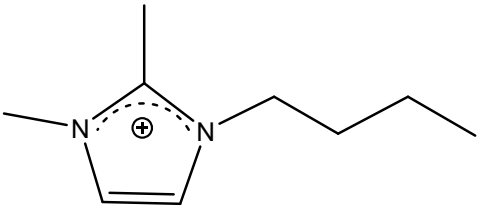

1-butyl-2,3-dimethylimidazolium

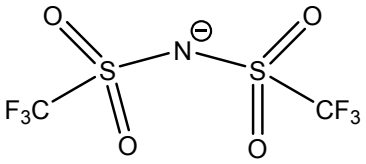

bis(trifluoromethanesulfonyl)imide

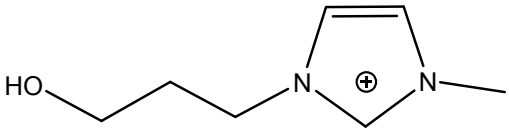

1-(3-hydroxypropyl)-3-methylimidazolium

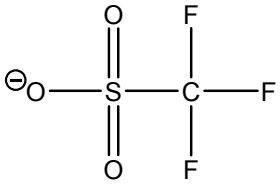

trifluoromethanesulfonate

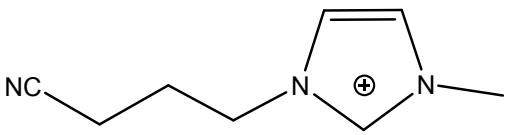

1-(3-cyanopropyl) -3-methylimidazolium

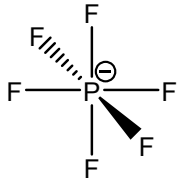

hexafluorophosphate

Figure S1.1. Structures of cations and anions of the studied ILs

1.1. 1-butyl-1-methylpyrrolidinium bromide, $[C_4C_1pyrr]Br$

In a two neck round bottom flask, 1-chlorobutane (221 ml, 2.05 mol) was added drop-wise, with cooling, to 1-methylpyrrolidine (200 ml, 1.92 mol) in ethyl acetate (200 ml). The mixture was stirred for 72 hours at 45 °C under nitrogen. The solution was then allowed to cool to -14 °C. A white crystalline precipitate was observed. The colourless solution was removed by cannula filtration and the white crystals were washed five times with ethyl acetate (5 x 50ml). The white crystals were dried *in vacuo* for 24h, affording $[C_4C_1pyrr]Br$.

Yield: 312.4 g (73.2%)

^{1}H-NMR δH (400MHz, DMSO-d_6): 3.52 (4H, m, CH_2-2 and CH_2-5), 3.31 (2H, m, NCH_2CH$_2$CH$_2$CH$_3$), 2.98 (3H, s, NCH_3), 2.09 (4H, s, CH_2-3 and CH_2-4), 1.67 (2H, m, NCH$_2$CH_2CH$_2$CH$_3$). 1.32 (2H, sextet, CH$_2$CH$_2$CH_2CH$_3$), 0.95 (3H, t, NCH$_2$CH$_2$CH$_2$CH_3).

^{13}C-NMR δC (400MHz, DMSO-d_6): 63.8 (N(CH_2)$_2$), 63.3 (N(CH$_2$)$_2$(CH_2)$_2$), 48.0 (NCH_3), 25.4 (NCH_2CH$_2$CH$_2$CH$_3$), 21.5 (NCH$_2$$CH_2CH_2CH_3$), 19.8 (NCH$_2CH_2$$CH_2CH_3$), 14.0 (NCH$_2CH_2CH_2$$CH_3$).

MS: (FAB)+ : m/z = 364, $[(C_4C_1pyrr)_2Br]^+$ 10%, and 142, $[C_4C_1pyrr]^+$, 100%,

MS: (FAB)- : m/z = 302, $[(C_4C_1pyrr)Br_2]^-$, 50%

1.2. 1-butyl-3-methylimidazolium chloride, $[C_4C_1im]Cl$

In a two neck round bottom flask, 1-chlorobutane (221 ml, 2.05 mol) was added drop-wise, with cooling, to 1-methylimidazole (200 ml, 2.51 mol) in ethyl acetate (200 ml). The mixture was allowed to reach room temperature and then was stirred at 70 °C with reflux for 72 hours under nitrogen. After cooling at -14 °C, a pale crystalline precipitate was observed. The upper layer was decanted and the solid was further purified by recrystallisation from acetonitrile. The white crystals were dried *in vacuo* for 24 h, affording $[C_4C_1im]Cl$.

Yield: 356.4 g (97%)

^{1}H NMR, δH (400MHz, DMSO-d_6): 9.08 (1H, s, CH-2), 8.01 (1H, s, CH-5), 7.92 (1H, s, CH-4), 4.23 (2H, t, NCH_2CH$_2$CH$_2$CH$_3$), 3.90 (3H, s, NCH$_3$), 1.77 (2H, quintet, NCH$_2$CH_2CH$_2$CH$_3$), 1.26 (2H, sextet, NCH$_2$CH$_2$CH_2CH$_3$), 0.86 (3H, t, NCH$_2$CH$_2$CH$_2$CH_3).

^{13}C NMR, δC (100MHz, DMSO-d_6): 136.92 (NCN), 122.42 and 124.01 (*C*-5 and *C*-4), 48.20 (NCH_2CH$_2$CH$_2$CH$_3$), 36.01 (NCH_3), 31.33 (NCH$_2$$CH_2CH_2CH_3$), 18.63 (NCH$_2CH_2$$CH_2CH_3$), 18.63 (NCH$_2CH_2$$CH_2CH_3$).

MS: (FAB)+: m/z = 313, $[(C_4C_1im)_2Cl]^+$ 5%, and 139, $[C_4C_1im]^+$, 100%,

MS: (FAB)- : m/z = 209, $[(C_4C_1im)Cl_2]^-$, 100% and 35, Cl^-, 55%

1.3. 1-Butyl-2,3-dimethylimidazolium chloride, $[C_4C_1C_1im]Cl$

As for the preparation of $[C_4C_1im]Cl$ (Section 1.2) except, chlorobutane (57.4 g (65.0 cm^3), 0.620 mol, 1.1 eq.) and 1,2-dimethylimidazole (54.2 g (50 cm^3), 0.564 mol, 1 eq.) used to afford $[C_4C_1C_1im]Cl$ as a colourless crystalline solid.

Yield: 89.1 g (83.8%)

^{1}H NMR, δH (400MHz, DMSO-d6): 7.78 and 7.53 (2H, s, 2NCH), 4.12 (2H, t, NCH$_2$(CH$_2$)$_2$CH$_3$), 3.73 (3H, s, NCH$_3$), 2.60 (3H, s, N2CCH$_3$), 1.74 (2H, quintet, NCH$_2$CH$_2$CH$_2$CH$_3$), 1.28 (2H, sextet, NCH$_2$CH$_2$CH$_2$CH$_3$) and 0.88 (3H, t, N(CH$_2$)$_3$CH$_3$);

^{13}C NMR, δC (400MHz, DMSO-d6): 144.36 (s, N2C), 122.21 and 120.76 (s, 2NCH), 47.37 (s, NCH$_2$(CH$_2$)$_2$CH$_3$), 34.50 (s, NCH$_3$), 31.19 (s, NCH$_2$CH$_2$CH$_2$CH$_3$), 18.88 (s, N(CH$_2$)$_2$CH$_2$CH$_3$), 13.31 (s, N(CH$_2$)$_3$CH$_3$) and 8.90 (s, N2CCH$_3$);

MS: (FAB)+: m/z = 342, $[(C_4C_1C_1im)_2Cl]^+$, 41%) and 153 ($[C_4C_1C_1im]^+$, 100)

MS: (FAB)- : m/z = 298, $[(C_4C_1C_1im)Cl_2]^-$, 100%

1.4. 1-butyl-1-methylpyrrolidinium *bis*(trifluoromethanesulfonyl)imide, $[C_4C_1pyrr][NTf_2]$

In a two neck round bottom flask containing a solution of $[C_4C_1pyrr]Br$ (72.7 g, 0.33 mol) in CH_2Cl_2 (150 ml), was added lithium *bis*(trifluoromethylsulfonyl)imide (94.0 g, 0.33 mol). The mixture was then stirred for 72 hours at room temperature under nitrogen. The mixture was then filtered using a cannula and the residual LiBr salt was washed with CH_2Cl_2 (3 x 50 ml). The combined organic extracts were washed with water until the aqueous phase was halide free (silver nitrate test). Then CH_2Cl_2 was removed by rotary evaporator. The liquid was stirred overnight with activated charcoal. The resulting liquid filtered through a pad of acidic alumina to give a colourless liquid $[C_4C_1pyrr][NTf_2]$.

Yield: 135.6 g (95.8%)

^{1}H-NMR, δH (400MHz, DMSO-d_6): 3.45 (4H, m, CH_2-2 and CH_2-5), 3.30 (2H, m, $NCH_2CH_2CH_2CH_3$), 2.98 (3H, s, NCH_3), 2.08 (4H, s, $NCH_2CH_2CH_2$), 1.69 (2H, m, $NCH_2CH_2CH_2CH_3$) 1.30 (2H, sextet, $NCH_2CH_2CH_2CH_3$), 0.93 (3H, t, $NCH_2CH_2CH_2CH_3$).

^{13}C-NMR δC (400 MHz, DMSO-d_6): 119.5 (CF_3), 63.42 ($N(CH_2)_2$), 62.96 ($N(CH_2)_2(CH_2)_2$), 47.98 (NCH_3), 24.91 ($NCH_2(CH_2CH_2CH_3)$, 21.04 ($NCH_2CH_2CH_2CH_3$), 19.27($N(CH_2)_2CH_2CH_3$), 13.3 ($N(CH_2)_3CH_3$).

MS: (FAB)+: m/z = 564, $[(C_4C_1pyrr)_2[NTf_2]]^+$ 5%, and 142, $[C_4C_1pyrr]^+$, 100%,

MS: (FAB)- : m/z = 702, $[(C_4C_1pyrr)[NTf_2]_2]^-$, 5%) and 280, $[NTf_2]^-$, 100%.

1.5. 1-butyl-3-methylimidazolium nitrate $[C_4C_1im][NO_3]$

Due to the fact that alkylnitrates are reactive and have a propensity to form explosive mixtures, extreme caution should be exercised when undertaking this reaction.

Butylnitrate (10.26g, 86mmol, 1.5eq) was mixed with ethylacetate (5mL). To this mixture a solution of ethylacetate (5mL) and methylimidazole (4.6mL, 57mmol, 1eq) was added dropwise with vigorous stirring. The solution was then refluxed for 24 hours, during which time a second liquid phase appeared. The mixture was cooled to -20 °C and white crystals of 1-butyl-3-methylimidazolium nitrate were collected.

Yield: 15.5g (89%)

^{1}H NMR, δH (400MHz, D_2O): 7.37 (1 H, d, C*H*-4), 7.31 (1 H, t, C*H*-5), 4.11 (2H, q, NCH_2CH_3), 3.79 (3 H, s, NCH_3), 1.39 (3 H, t, NCH_2CH_3).

^{13}C NMR, δC (100MHz, D_2O): 123.33 (s, *C*H-4), 121.74 (s, *C*H-5), 44.69 (1 H, s, NCH_2CH_3), 35.46 (s, NCH_3), 14.35 (s, NCH_2CH_3).

MS: (FAB)+: m/z = 139, $[C_4C_1im]^+$, 100%

MS: (FAB)- : m/z = 62, $[NO_3]^-$, 30%

1.1. 1-butyl-3-methylimidazolium thiocyanate$[C_4C_1im][SCN]$

1-butyl-3-methylimidazolium chloride (2.09g, 11.96mmol, 1eq) in acetonitrile (15mL) was mixed with barium thiocyanate (1.84g, 5.98mmol, 0.5eq) in acetonitrile (15mL) and the solution was stirred for 4 hours. A white precipitate was formed. The suspension was centrifuged and the liquor decanted. The solvent was removed yielding a slightly pink liquid 1-butyl-3-methylimidazolium thiocyanate.

Yield: 1.86g (79%).

^{1}H NMR, δH (400MHz, DMSO-d6): 9.30ppm (1H, s, C*H*-2), 7.82ppm (1H, s, C*H*-4), 7.75ppm (1H, s, C*H*-5), 4.19ppm (2H, t, $NCH_2CH_2CH_2CH_3$), 3.87ppm (3H, s, NCH_3), 1.77ppm (2H, quintet, $NCH_2CH_2CH_2CH_3$), 1.27ppm (2H, sextet, $N(CH_2)_2CH_2CH_3$), 0.90ppm (3H, t, $N(CH_2)_3CH_3$).

^{13}C NMR (400MHz, $CDCl_3$): 136.67ppm (C(2)H). 131.66ppm (SCN), 23.85ppm (C(4)H), 22.30ppm (C(5)H), 50.11ppm ($NCH_2(CH_2)_2CH_3$), 36.78ppm (NCH_3), 32.09ppm ($NCH_2CH_2CH_2CH_3$), 19.52ppm ($N(CH_2)_2CH_2CH_3$), _ = 13.48ppm ($N(CH_2)_3CH_3$).

MS: (FAB)+: m/z = 139, $[C_4C_1im]^+$ 100%,

MS: (FAB)- : m/z = 26, $[CN]^-$ 95%, 32, S^- 94%, and 58, SCN^- 100%.

1.2. 1-butyl-3-methylimidazolium *bis*(trifluoromethanesulfonyl)imide, $[C_4C_1im][NTf_2]$

In a two neck round bottom flask, lithium *bis*(trifluoromethylsulfonyl)imide (103.3 g, 0.35 mol) and $[C_4C_1im]Cl$ (60.0 g, 0.34 mol) were mixed and stirred in CH_2Cl_2 (150 ml) for 72 hours at room temperature under nitrogen. The mixture was then filtered using a cannula and the residual LiCl salt was washed with CH_2Cl_2 (3 x 50 ml). The combined organic extraction was washed with water until the aqueous phase was halide free (silver nitrate test). The CH_2Cl_2 was then removed by a rotary evaporator. The resulting liquid was treated with activated charcoal and filtered through a pad of acidic alumina to give the colourless liquid $[C_4C_1im][NTf_2]$.

Yield: 132.5 g (93%)

^{1}H NMR, δH (400MHz, DMSO-d_6): 9.10 (1H, s, C*H*-2), 7.74 (1H, s, C*H*-5), 7.67 (1H, s, C*H*-4), 4.17 (2H, t, NC*H*$_2$CH$_2$CH$_2$CH$_3$), 3.86 (3H, s, NCH$_3$), 1.78 (2H, quintet, NCH$_2$C*H*$_2$CH$_2$CH$_3$), 1.28 (2H, sextet, NCH$_2$CH$_2$C*H*$_2$CH$_3$), 0.91 (3H, t, NCH$_2$CH$_2$CH$_2$C*H*$_3$).

^{13}C NMR, δC (400MHz, DMSO-d_6): 136.92 (N*C*N), 124.01 and 122.64 (*C*-5 and *C*-4), 121.52 (*C*F$_3$), 48.95 (N*C*H$_2$CH$_2$CH$_2$CH$_3$), 36.01 (N*C*H$_3$), 31.75 (NCH$_2$*C*H$_2$CH$_2$CH$_3$), 19.15 (NCH$_2$CH$_2$*C*H$_2$CH$_3$), 13.45 (NCH$_2$CH$_2$*C*H$_2$CH$_3$).

MS: (FAB)+: m/z = 558, $[(C_4C_1im)_2[NTf_2]]^+$ 5%, and 142, $[C_4C_1im]^+$, 100%,

MS: (FAB)- : m/z = 280, $[NTf_2]^-$, 100%.

1.3. 1-butyl-1-methylimidazolium trifluoromethanesulfonate, $[C_4C_1im][OTf]$

In a two neck round bottom flask, lithium trifluoromethanesulfonate (33.5 g, 0.33 mol) and $[C_4C_1im]Cl$ (55.7 g, 0.32 mol) were mixed and stirred in CH_2Cl_2 (80 ml) for 72 hours under an inert atmosphere at room temperature. The mixture was then filtered using a cannula and the residual LiCl salt was washed with CH_2Cl_2 (3 x 50 ml). The solution was diluted with CH_2Cl_2 (700 ml) and washed many times with water (1.0 ml) until the solution was halide free by silver nitrate test. The CH_2Cl_2 was removed using rotary evaporator. The resulting liquid was treated with activated charcoal and filtered through a pad of acidic alumina to give colourless liquid $[C_4C_1im][OTf]$.

Yield: 82.4 g (86.7%)

^{1}H NMR, δH (400MHz, DMSO-d6): 9.10 (1H, s, C*H*-2), 7.76 (1H, s, C*H*-5), 7.67(1H, s, C*H*-4), 4.16 (2H, t, NC*H*$_2$CH$_2$CH$_2$CH$_3$), 3.85 (3H, s, NCH$_3$), 1.76 (2H, quintet, NCH$_2$C*H*$_2$CH$_2$CH$_3$), 1.26 (2H, sextet, NCH$_2$CH$_2$C*H*$_2$CH$_3$), 0.88 (3H, t, NCH$_2$CH$_2$CH$_2$C*H*$_3$).

^{13}C NMR, δC (400MHz, DMSO-d6): 136.92 (N*C*N), 124.01 and 122.64 (*C*-5 and *C*-4), 119.53 (*C*F$_3$), 48.80 (N*C*H$_2$CH$_2$CH$_2$CH$_3$), 35.90 (N*C*H$_3$), 31.60 (NCH$_2$*C*H$_2$CH$_2$CH$_3$), 18.97 (NCH$_2$CH$_2$*C*H$_2$CH$_3$), 13.35 (NCH$_2$CH$_2$*C*H$_2$CH$_3$).

MS: (FAB)+: m/z = 427, $[(C_4C_1im)_2[OTf]]^+$ 20%, and 139, $[C_4C_1im]^+$, 100%,

MS: (FAB)- : m/z = 437, $[(C_4C_1im)(OTf)_2]^-$, 22% and 149, $[OTf]^-$, 100%.

1.4. 1-butyl-1-methylimidazolium hexafluorophosphate, $[C_4C_1im][PF_6]$

In a two neck round bottom flask, lithium hexafluorophosphate (35.0 g, 0.23 mol) and $[C_4C_1im]Br$ (50 g, 0.23 mol) were mixed and stirred in CH_2Cl_2 (150 ml) for 72 hours at room temperature under nitrogen. The mixture was then filtered using cannula and the residual LiBr salt was washed with CH_2Cl_2 (3 x 50 ml). The combined organic extraction was washed with water until the aqueous phase was halide free by silver nitrate test. The CH_2Cl_2 was then removed by a rotary evaporator. The resulting liquid was treated with activated charcoal and filtered through a pad of acidic alumina to give the colourless liquid $[C_4C_1im][PF_6]$.

Yield: 54.6 g (83.5%)

^{1}H NMR, δH (400MHz, DMSO-d6): 9.05 (1H, s, C*H*-2), 7.72 (1H, s, C*H*-5), 7.65(1H, s, C*H*-4), 4.16 (2H, t, NC*H*$_2$CH$_2$CH$_2$CH$_3$), 3.84 (3H, s, NCH$_3$), 1.77 (2H, q, NCH$_2$C*H*$_2$CH$_2$CH$_3$), 1.27 (2H, sextet, NCH$_2$CH$_2$C*H*$_2$CH$_3$), 0.86 (3H, t, NCH$_2$CH$_2$CH$_2$C*H*$_3$).

^{13}C NMR, δC (400MHz, DMSO-d6): 136.55 (N*C*N), 123.62 and 122.26 (*C*-5 and *C*-4), 48.62 (N*C*H$_2$CH$_2$CH$_2$CH$_3$), 35.70 (N*C*H$_3$), 31.39 (NCH$_2$*C*H$_2$CH$_2$CH$_3$), 18.81 (NCH$_2$CH$_2$*C*H$_2$CH$_3$), 18.22 (NCH$_2$CH$_2$*C*H$_2$CH$_3$).

MS: (FAB)+: m/z = 423, $[(C_4C_1im)_2[PF_6]]^+$ 22%, and 139, $[C_4C_1im]^+$, 100%,

MS: (FAB)- : m/z = 429, $[(C_4C_1im)[PF_6]_2]^-$, 30%) and 145, $[PF_6]^-$, 100%.

1.5. 1-(3-hydroxypropyl)-3-methylimidazolium chloride $[(HO)^3C_3C_1im]Cl$

In a two neck round bottom flask, containing 1-methylimidazole (100 ml, 1.19 mol) in toluene (100 ml), 3-chloro-1-propanol (80 ml, 1.00 mol) was added dropwise, with cooling. The mixture was allowed to reach room temperature and then was stirred at 60 °C for 10 days under nitrogen. After cooling at -14 °C, a pale crystalline precipitate was observed. The upper layer was decanted and the solid was washed 3 times with dry ethyl acetate (50 ml). The solid was then further purified by recrystallisation from acetonitrile. The white crystals were dried *in vacuo* for 24 h, affording $[(HO)^3C_3C_1im]Cl$.

Yield: 152.4 g (86.5%)

^{1}H NMR, δH (400MHz, DMSO-d6): 9.40 (1H, s, C*H*-2), 7.85 (1H, s, C*H*-5), 7.65 (1H, s, C*H*-4), 5.0 (1H, s, O*H*), 4.30 (2H, t, $NCH_2CH_2CH_2OH$), 3.90 (3H, s, NCH_3), 3.50 (2H, t, $NCH_2CH_2CH_2OH$), 3.33 (2H, t, $NCH_2CH_2CH_2OH$), 1.93 (2H, quintet, $NCH_2CH_2CH_2CH_3$).

^{13}C NMR, δC (100MHz, DMSO-d6): 137.35 (N*C*N), 123.95 and 122.85 (*C*-5 and *C*-4), 57.20 ($NCH_2CH_2CH_2CH_3$), 36.01 (NCH_3), 31.33 ($NCH_2CH_2CH_2CH_3$), 18.63 ($NCH_2CH_2CH_2CH_3$), 18.63 ($NCH_2CH_2CH_2CH_3$).

MS: (FAB)+: m/z = 317, $[(HO)^3C_3C_1im)_2Cl]^+$ 50%, and 141, $[(HO)^3C_3C_1im]^+$,100%

MS: (FAB)- : m/z = 35, Cl-, 100%, and 211, $[(HO)^3C_3C_1im)Cl_2]^-$ 100%.

1.6. 1-(3-hydroxypropyl)-3-methylimidazolium *bis*(trifluoromethanesulfonyl)imide $[(HO)^3C_3C_1im][NTf_2]$

In a two neck round bottom flask, lithium *bis*(trifluoromethylsulfonyl)imide (103.3 g, 0.35 mol) and $[(HO)^3C_3C_1im]Cl$ (60.0 g, 0.34 mol) were mixed and refluxed in a mixture of CH_2Cl_2 and water (200 ml) for 72 hours. The mixture was then filtered using a canula and the residual LiCl salt was washed with CH_2Cl_2 (3 x 50 ml). The combined organic extraction was washed with water until the aqueous phase was halide free (silver nitrate test). The resulting liquid was treated with activated charcoal and filtered through a pad of neutral alumina to give the colourless liquid $[(HO)^3C_3C_1im][NTf_2]$.

Yield: 127.5 g (89.1%)

^{1}H NMR, δH (400MHz, DMSO-d6): 9.40 (1H, s, C*H*-2), 7.85 (1H, s, C*H*-5), 7.65 (1H, s, C*H*-4), 5.0 (1H, s, O*H*), 4.30 (2H, t, $NCH_2CH_2CH_2OH$), 3.90 (3H, s, NCH_3), 3.50 (2H, t, $NCH_2CH_2CH_2OH$), 3.33 (2H, t, $NCH_2CH_2CH_2OH$), 1.93 (2H, quintet, $NCH_2CH_2CH_2CH_3$).

^{13}C NMR, δC (100MHz, DMSO-d6): 137.35 (N*C*N), 123.95 and 122.85 (*C*-5 and *C*-4), 120.01 (CF_3), 57.20 ($NCH_2CH_2CH_2CH_3$), 36.01 (NCH_3), 31.33 ($NCH_2CH_2CH_2CH_3$), 18.63 ($NCH_2CH_2CH_2CH_3$), 18.63 ($NCH_2CH_2CH_2CH_3$).

MS: (FAB)+: m/z = 141, $[(HO)^3C_3C_1im]^+$, 100%,

MS: (FAB)- : m/z = 280, $[NTf_2]^-$, 100%.

1.7. 1-(3-cyanopropyl) -3-methylimidazolium chloride $[(CN)^4C_3C_1im]Cl$

In a two neck round bottom flask, containing 1-methylimidazole (80 ml, 1.00 mol) in ethyl acetate (100 ml), 4-chlorobutyronitrile (96.6 ml, 1.02 mol) was added drop-wise, with cooling. The mixture was allowed to reach room temperature and then was refluxed at 80 °C for 3 days under nitrogen. After cooling at -14 °C, a pale crystalline precipitate was observed. The upper layer was decanted and the solid was washed 3 times with dry ethyl acetate (50 ml). The solid was then further purified by recrystallisation from acetonitrile. The white crystals were dried *in vacuo* for 24 h, affording $[(CN)^3C_3C_1im]Cl$.

Yield: 114.9 g (62.1%)

^{1}H NMR, δH (400MHz, DMSO-d6): 9.17 (1H, s, C*H*-2), 7.80 (1H, s, C*H*-5), 7.74 (1H, s, C*H*-4), 4.24 (2H, t, $NCH_2CH_2CH_2CN$), 3.85 (3H, s, NCH_3), 2.59 (2H, t, $NCH_2CH_2CH_2CN$). 2.15 (2H, quintet, $NCH_2CH_2CH_2CN$).

^{13}C NMR, δC (100MHz, DMSO-d6): 138.0 (N*C*N), 124.01 and 122.54 (*C*-5 and *C*-4), 121.52 (*C*N), 120.0 (CF_3) 48.00 ($NCH_2CH_2CH_2CN$), 36.01 (NCH_3), 25.55 ($NCH_2CH_2CH_2CN$), 13.45 ($NCH_2CH_2CH_2CN$).

MS: (FAB)+: m/z = 335, $[(CN)^3C_4C_1im)_2Cl]^+$ 50%, and 150, $[(CN)^3C_4C_1im]^+$, 100%

MS: (FAB)- : m/z = 35, Cl^-, 50%, and 220, $[(CN)^3C_4C_1im)Cl_2]^-$ 100%.

1.8. 1-(3-cyanopropyl)-3-methylimidazolium *bis*(trifluoromethanesulfonyl)imide $[(CN)^3C3C_1im][NTf_2]$

In a two neck round bottom flask, lithium *bis*(trifluoromethylsulfonyl)imide (103.3 g, 0.35 mol) and $[(CN)^3C_4C_1im]Cl$ (63.0 g, 0.34 mol) were mixed and stirred in CH_2Cl_2 (150 ml) for 72 hours at room temperature under nitrogen. The mixture was then filtered using a canula and the residual LiCl salt was washed with CH_2Cl_2 (3 x 50 ml). The combined organic extraction was washed with water until the aqueous phase was halide free (silver nitrate test). The CH_2Cl_2 was then removed by a rotary evaporator. The resulting liquid was treated with activated charcoal and filtered through a pad of acidic alumina to give the colourless liquid $[(CN)^3C_3C_1im][NTf_2]$.

Yield: 136.2 g (93.2%)

^{1}H NMR, δH (400MHz, DMSO-d6): 9.30 (1H, s, C*H*-2), 7.76 (1H, s, C*H*-5), 7.74 (1H, s, C*H*-4), 4.15 (2H, t, $NCH_2CH_2CH_2CN$), 3.86 (3H, s, NCH_3), 2.60 (2H, t, $NCH_2CH_2CH_2CN$). 2.30 (2H, quintet, $NCH_2CH_2CH_2CN$).

^{13}C NMR, δC (100MHz, DMSO-d6): 137.5 (N*C*N), 124.01 and 122.54 (*C*-5 and *C*-4), 121.52 (*C*N), 120.0 (CF_3) 48.00 ($NCH_2CH_2CH_2CN$), 36.01 (NCH_3), 26.01 ($NCH_2CH_2CH_2CN$), 13.45 ($NCH_2CH_2CH_2CN$).

MS: (FAB)+: m/z = 150, $[(CN)^3C_3C_1im]^+$, 100%,

MS: (FAB)- : m/z = 280, $[NTf_2]^-$, 100%.

1.9. 1-butyl-2,3-dimethylimidazolium bis(trifluoromethanesulfonyl)imide, $[C_4C_1C_1im][NTf_2]$

To a flask containing a stirred solution of $[C_4C_1C_1im]Cl$ (30.9 g, 0.164 mol, 1 eq.) in CH_2Cl_2 (50 cm^3) under N_2 was added $Li[NTf_2]$ (48.8 g, 0.169 mmol, 1.03 eq.). The mixture was stirred for 24 h under N_2 and the colourless precipitate allowed to settle. Cannula filtration and subsequent rinsing of the NaCl residue with CH_2Cl_2 (2 × 50 cm^3) gave a colourless liquid, which was further diluted with CH_2Cl_2 (100 cm^3) and washed with aliquots of water (3 × 20 ml) until halide free, as indicated by the $AgNO_3$ test. The liquid was dried *in vacuo* for 3 h at 80 °C then filtered through a short pad of neutral alumina (*l* = 1−1.5 cm) and thoroughly dried *in vacuo* at 80 °C for a further 8 h to afford $[C_4C_1C_1im][NTf_2]$ as a free-flowing colourless liquid;

Yield: 71.0 g, (89.0%)

^{1}H NMR, δH (400MHz, DMSO-d6): 7.58 (2H, AB quartet, 2NC*H*), 4.12 (2H, t, $NCH_2(CH_2)_2CH_3$), 3.77 (3H, s, NCH_3), 2.59 (3H, s, N_2CCH_3), 1.73 (2H, quintet, $NCH_2CH_2CH_2CH_3$), 1.32 (2H, sextet, $NCH_2CH_2CH_2CH_3$) and 0.92 (3H, t, $N(CH_2)_3CH_3$);

^{13}C NMR, δC (400MHz, DMSO-d6): 144.17 (s, N_2C), 122.26 and 120.80 (s, 2N*C*H), 119.57 (q, $[NSO_2CF_3]^-$), 47.44 (s, $NCH_2(CH_2)_2CH_3$), 34.51 (s, NCH_3), 31.16 (s, $NCH_2CH_2CH_2CH_3$), 18.85 (s, $N(CH_2)_2CH_2CH_3$), 13.06 (s, $N(CH_2)_3CH_3$) and 8.92 (s, N_2CCH_3);

MS: (FAB)+: m/z = 586,$[(C_4C_1C_1im)_2NTf_2]^+$, 20% and 153, $[C_4C_1C_1im]^+$, 100%;

MS: (FAB)- : m/z = 280, $[NTf_2]^-$, 100%.

1.10. 1-butyl-2,3-dimethylimidazolium hexafluorophosphate, $[C_4C_1C_1im][PF_6]$

In a two neck round bottom flask, lithium hexafluorophosphate (35.0 g, 0.23 mol) and $[C_4C_1C_1im]Cl$ (43.3 g, 0.23 mol) were mixed and stirred in CH_2Cl_2 (150 ml) for 72 hours at room temperature under nitrogen. The mixture was then filtered using a cannula and the residual LiCl salt was washed with CH_2Cl_2 (3 x 50 ml). The combined organic extraction was washed with water until the aqueous phase was halide free by silver nitrate test. The CH_2Cl_2 was then removed by a rotary evaporator. The resulting liquid was treated with activated charcoal and filtered through a pad of acidic alumina to give the colourless liquid $[C_4C_1C_1im][PF_6]$.

Yield: 60.3 g (87.5%)

^{1}H NMR, δH (400MHz, DMSO-d6): 9.05 (1H, s, C*H*-2), 7.72 (1H, s, C*H*-5), 7.65(1H, s, C*H*-4), 4.16 (2H, t, NC*H*$_2$CH$_2$CH$_2$CH$_3$), 3.84 (3H, s, NCH$_3$), 2.58 (3H, s, N$_2$CC*H*$_3$), 1.77 (2H, q, NCH$_2$C*H*$_2$CH$_2$CH$_3$), 1.27 (2H, sextet, NCH$_2$CH$_2$C*H*$_2$CH$_3$), 0.86 (3H, t, NCH$_2$CH$_2$CH$_2$C*H*$_3$).

^{13}C NMR, δC (400MHz, DMSO-d6): 136.55 (N*C*N), 123.62 and 122.26 (*C*-5 and *C*-4), 48.62 (N*C*H$_2$CH$_2$CH$_2$CH$_3$), 35.70 (N*C*H$_3$), 31.39 (NCH$_2$*C*H$_2$CH$_2$CH$_3$), 18.81 (NCH$_2$CH$_2$*C*H$_2$CH$_3$), 18.22 (NCH$_2$CH$_2$*C*H$_2$CH$_3$) and 8.97 (s, N2C*C*H$_3$)

MS: (FAB)+: m/z = 453, [(C$_4$C$_1$C$_1$im)$_2$PF$_6$]$^+$ 24%, and 154, [C$_4$C$_1$C$_1$im]$^+$, 100%,

MS: (FAB)- : m/z = 444, [(C$_4$C$_1$C$_1$im)(PF$_6$)$_2$]$^-$, 26% and 145, [PF$_6$]$^-$, 100%.

Section 2: Synthesis of [Cu(acac)(tmen)]+ complexes

2.1 (Acetylacetonato)(N,N,N',N',-tetramethylethylenediamine)copper(II) nitrate, [Cu(acac)(tmen)][NO$_3$]

Cu(NO$_3$)$_2$x3H$_2$O (2.08 g, 8.6 mmol) was stirred in solution of a minimum of aqueous ethanol (1:1 v/v). AcacH (0.9 ml, 8.8 mmol) and tmen (1.3 ml, 8.8 mmol) were combined, resulting in an inky, dark blue liquid. Anhydrous sodium carbonate was added to neutralize the acacH, which caused some frothing. The solution was filtered and the solvent was removed on a water bath from the residual dark blue liquid. The crude product was then recrystallised from ethanol to give dark blue-violet needles.

Yield: 2.765 g, 94%.

Melting point: 160 ^{o}C.

IR (ATR) υ_{max}/cm^{-1}: 1589 and 1525 (C=C + C=O), 1342 (N-O), 1349 (C-N), 1276 and 1025 (NO$_3$), 975 (C=C + C=O), 810 (NO$_3$)

MS: (FAB+): m/z = 278, [Cu(acac)(tmen)]$^+$, 100%, 179, [Cu(tmen)]$^+$, 28%

MS: (FAB-): m/z = 62, [NO$_3$]$^-$, 100%

2.2 (Acetylacetonato)(N,N,N',N',-tetramethylethylenediamine)copper(II) trifluoromethanesulfonate, [Cu(acac)(tmen)][OTf]

In a schlenk flask under nitrogen, sodium trifluromethanesulfonate (1.68 g, 10 mmol) was slurried in dry DCE (8 ml), [Cu(acac)(tmen)][NO$_3$] (3.4 g, 8 mmol) in dry DCE (8 ml) was added *via* cannula with vigorous stirring. After 8 hours stirring, a pale solid was observed beneath the dark blue mixture. The mixture was filtered and solvent was removed from the dark blue filtrate. The sparkly dark blue crude product was then recrystallised from a mixture of hexane and butanol (6:1 v/v) to give a dark blue plate like crystals.

Yield: 2.965 g, 86%.

Melting point: 115 ^{o}C.

IR (ATR) υ_{max}/cm^{-1}: 1592 and 1520 (C=C + C=O), 1375 (N-O), 1276 (C-N) 1243 (S=O), 1024 (C-F), 953 (C=C + C=O).

MS: (FAB+): m/z = 278, [Cu(acac)(tmen)]$^+$, 100%, 179, [Cu(tmen)]$^+$, 10%

MS: (FAB-): m/z = 149, [OSO$_2$CF$_3$]$^-$, 100%

2.3 (Acetylacetonato)(N,N,N',N',-tetramethylethylenediamine)copper(II) hexafluorophosphate, [Cu(acac)(tmen)][PF6]

As for the preparation of [Cu(acac)(tmen)][OTf] except, potassium hexafluorophosphate (1.78 g, 10 mmol) was slurried in 8 ml of dry dce. [Cu(acac)(tmen)][NO$_3$] (3.4 g, 8 mmol) was added to afford [Cu(acac)(tmen)][PF$_6$]. Recrystallisation from a mixture of hexane and butanol (1:1 v/v) yielded a red-purple crystalline powder.

Yield: 1.9023g, 56%.

Melting point: 145 ^{o}C.

IR (ATR) υ_{max}/cm^{-1}: 1579 and 1525 (C=C + C=O), 1283 (C-N), 952 (C=C +C=O), 838 (P-F)

MS: (FAB+): m/z = 278, [Cu(acac)(tmen)]$^+$, 100%

MS: (FAB-): m/z = 145, [PF$_6$]$^-$, 100%

2.4 (Acetylacetonato)(N,N,N',N',-tetramethylethylenediamine)copper(II) bis(trifluoromethanesulfonyl)imide, [Cu(acac)(tmen)][NTf2]

As for the preparation of [Cu(acac)(tmen)][OTf] except, lithium *bis*(trifluoromethanesulfonyl)imide (1.53 g, 5 mmol) was slurried in dry dce (6 ml). [Cu(acac)(tmen)][NO_3] (1.7 g, 4 mmol) was added to afford [Cu(acac)(tmen)][NTf_2]. Recrystallisation was from a mixture of hexane and butanol (4:1 v/v), yielding an analytically pure purple fine crystalline powder.

Yield: 1.563 g, 70%.

Melting point: 95 ^oC.

IR (ATR) υ_{max}/cm^{-1}: 1591 and 1524 (C=C + C=O), 1346 and 1186 (N-SO_2), 1224 , 1136 (C-F), 1055 (S-O), 952 (C=C + C=O).

MS: (FAB+): m/z = 278, $[Cu(acac)(tmen)]^+$, 100%, 179, $[Cu(tmen)]^+$, 40%, 115, $[tmen]^+$, 50%

MS: (FAB-) : m/z = 280, $[NTf_2]^-$, 100%

2.5 (Acetylacetonato)(N,N,N',N',-tetramethylethylenediamine)copper(II) chloride, [Cu(acac)(tmen)]Cl

As for the preparation of [Cu(acac)(tmen)][NO_3] except, copper(II) chloride dihydrate (1.04 g, 8.6 mmol) was stirred in a minimum volume of aqueous ethanol (1:1 v/v). AcacH (0.9 ml, 8.8 mmol) and tmen (1.3 ml, 8.8 mmol) [Cu(acac)(tmen)][NO_3] (1.7 g, 4 mmol) was added to afford [Cu(acac)(tmen)]Cl. Recrystallisation from a mixture of dichloromethane and hexane (1:1 v/v) yielded an analytically pure green powder.

Yield: 2.563 g, 95%.

Melting point: 125 ^oC

IR (ATR) υ_{max}/cm^{-1}: 1586 (C=C + C=O str.), 1521 (C=C + C=O str.), 952 (C=C + C=O str.).

MS: (FAB+): m/z = 278, $[Cu(acac)(tmen)]^+$, 100%

MS: (FAB-): m/z = 35, Cl^-, 100%

2.6 (Acetylacetonato)(N,N,N',N',-tetramethylethylenediamine)copper(II) thiocyanate, [Cu(acac)(tmen)][SCN]

As for the preparation of [Cu(acac)(tmen)][OTf] except, sodium thiocyante (4.05 g, 5 mmol) was slurried in dry dce (6 ml). [Cu(acac)(tmen)][NO_3] (1.7 g, 4 mmol) was added to afford [Cu(acac)(tmen)][SCN]. Recrystallisation from dichloromethane yielded an analytically pure dark green solid.

Yield: 1.423g, 70%.

IR (ATR) υ_{max}/cm^{-1}: 2071 (SCN), 1591 and 1524 (C=C + C=O), 806, 732 (SCN)

MS: (FAB+): m/z = 278, $[Cu(acac)(tmen)]^+$, 100%, 179, $[Cu(tmen)]^+$, 40%, 115, $[tmen]^+$, 35%

MS: (FAB-): m/z = 58, $[SCN]^-$, 50%, 179, $[(Cu)(SCN)_2]^-$, 100%

2.7 (Acetylacetonato)(N,N,N',N',-tetramethylethylenediamine)copper(II) perchlorate, [Cu(acac)(tmen)][ClO_4]

Acetylacetone (2.0 mmol) and NH_3 (2.0 mmol) in 10 ml of ethanol were combined with 10 cm^3 ethanol solution of $Cu(ClO_4)_2x6H_20$ (2.0 mmol), and stirred for 30 min before the addition of tmen (2.0 mmol) solution in ethanol. After reaction at room temperature for 3 h, diethyl ether was added to the resulting solution to give purple crystals. The product was recrystallized from dichloromethane and ether.

Yield, 85%.

Melting point: 184 °C

IR (ATR) υ_{max}/cm^{-1}: 1591 and 1524 (C=C + C=O), 952 (C=C + C=O).

MS: (FAB+): m/z = 278, $[Cu(acac)(tmen)]^+$, 100%, 179, $[Cu(tmen)]^+$, 40%, 115, $[tmen]^+$, 35%

MS: (FAB-): m/z = 99, $[ClO_4]^-$, 80% and 261, $[(Cu)(ClO_4)_2]^-$, 100%

Synthesis of Cu(sacsac)2

Firstly acethylacetone (4 g, 40 mmol) was thionated by 24h reflux in 15 ml of acetonitrile and P_2S_5/Al_2O_3 (1.36g) to yield sacsacH in the form of dark crystals.[1] Reaction completion was monitored with TLC.

Solutions in minimum water of $Cu(NO_3)_2.3H_2O$ (1.2 g, 5 mmol) and sacsacH (1.32g, 10mmol) were combined, resulting in a brown solution. Aqueous NaOH (0.40 g, 10mmol) was added giving a grey-blue mixture. Filtration removed a brown solid from a dark filtrate. Recrystallisation from acetone gave a brown powder.

Yield: 0.69 g (42%).

Melting point: 103 °C

IR (ATR) υ_{max}/cm^{-1}= 3207 (C=C), 2922 (CH_3), 1612, 1430 (C=C), 1124 (C=S), 962, 668 (CH).

Section 3: General Computational Details

All calculations have been carried out using the Gaussian 09 suite of programs (revision D.01).[2] Structures fully optimised under no symmetry constraints. A pruned numerical integration grid of 99 radial shells and 590 angular points per shell was employed in conjunction with convergence criteria of 10^{-9} on the density matrix and 10^{-7} on the energy matrix. Frequency analysis has been performed for each structure to confirm it as a minimum.

Individual anions have been optimised at the B3LYP-D3BJ/6-311+G(d,p) level. Population analysis has been carried out using the NBO method (version 5.9)[3] and the electrostatic potential derived charges calculated employing the CHELPG scheme.[4,5] ChelpG charges for the anions were constrained to fit the dipole moment of the whole molecule. No default van der Waals radius is implemented for copper in the CHELPG method, requiring a value for the radius of copper to be specified by the user. A radius of of 2.00 Å was employed here for the copper centres, default radii were employed for all other elements. A radius of 2.00 Å has previously been shown to be a justifiable choice for ESP schemes.[6]

TM systems are a difficult proposition for DFT, this is exacerbated by the multi-configurational nature of systems that undergo Jahn-Teller distortion. These calculations are presented as a computational study, but cannot be assumed to represent quantitative accuracy, and may even be qualitatively incorrect. Nevertheless, there are numerous examples of such calculations in the literature.

A detailed MO analysis was carried out for the $[Cu(acac)(tmen)]^+$ cation in the gas phase. Both unrestricted and restricted open shell calculations were performed using the B3LYP functional in conjunction with an aug-cc-pVTZ basis set for the first row heavy atoms and a cc-pVTZ basis set for the H-atoms. The Cu-atom was modelled using a scalar relativistic Stuttgart PP (ECP10MWB) and the associated basis set. Four selected copper complexes were examined using DFT (M06, M06HF and M06L) with an aug-cc-pVDZ basis set, charges were determined using CHelpG.

UV-Vis spectra are notoriously dependent on the quantity of exchange included, thus we have tested the range of functionals that include 0-100% of exchange. The M06 group of functionals have been employed, these include M06, M06-L, M06-HF and M06-2L.[3] The M06-2X (54% exchange) functional has been parameterized only for non-metals and is not of interest here. M06-HF has full (100%) HF exchange (and thus is poor for TMs but good for charge transfer states) and M06-L is constrained to be local. Both M06 (27% exchange) and M06-L (0% exchange) have been identified as suitable functionals for organometallic applications; M06 is recognised as a functional with broad applicability, while M06-L may offer improved accuracy for transition metals.[7] M06 performs well for valence excitations, M06 and M06-L perform well for metal cation excitations.[3,8] In contrast, B3LYP includes 20% exchange.

[Cu(acac)(tmen)]+ cation structures were initially optimised (multiplicity 2, unrestricted spin) in the gas-phase using the M06 density functional[3] in conjunction with the aug-cc-pVDZ basis set. Each of the copper complexes was subsequently optimised employing the related M06-HF and M06-L density functionals,[9] also in conjunction with the aug-cc-pVDZ basis. The gas phase calculation provides the best system to study when no external influences are present, however the experimental data must be obtained in the solid or liquid phase. To test the influence of the solvent on the calculation our selected functionals (B3LYP, M06 and M06L) have been tested employing a generalised solvent model SMD[10] parameterised for the least interacting IL studied here $[C_4C_1im][PF_6]$ with the following

parameters: eps=11.4 epsinf=1.985281 HBondAcidity=0.266 HBondBasicity=0.216 SurfaceTensionAtInterface=70.24 CarbonAromaticity=0.1765 ElectronegativeHalogenicity=0.3529.

Subsequently a TD-DFT calculation of the 25 lowest excited states (multiplicity 2, unrestricted spin) were carried evaluated to determine the UV-Vis spectra.

Four selected copper complexes with alternative ligands were further examined. In addition to $[Cu(acac)_2]$, the methyl R groups of acac were replaced with CF_3 forming $[Cu(hfac)_2]$ and the oxygen atoms of acac were replaced with sulphur forming a dithioacetylacetone complex $[Cu(sacsac)_2]$. Structures were optimised employing the M06 and M06-L functionals with an aug-cc-pVDZ basis set and charges were evaluated using both orbital (NBO) and electrostatic potential (CHelpG) based methods.

Section 4: Isolated $[Cu(acac)(tmen)]^+$ MO analysis and computed UV-Vis Spectra

4.1 MO analysis

Under a standard MO analysis for an octahedral complex the MO diagram includes nd (n+1)s and (n+1)p AOs on the metal and the ligand donor orbitals. Combining fragment orbitals of the correct symmetry provides the non-bonding dxz, dyz and dxy (t_{2g} MOs) and the bonding and antibonding combinations of the dx^2-y^2 and dz^2 (e_g MOs), the orbitals associated with the dAO manifold (relating to crystal field theory CFT) are the antibonding metal-ligand antibonding e_g MOs. The tetragonal distortion reduces the symmetry to D_{4h} and allows the (previously spherical symmetry) 4s and dz_2 MOs to mix (as they both now have a_{1g} symmetry) giving rise to the well-known Jahn-Teller distortion of Cu(II) complexes, **ESI Figure S4.1.1**. The resulting orbital pattern is of a partially occupied, high energy heavily 4s/dz^2 mixed ligand antibonding a_{1g} MO lying well above the non-bonding e_g (d_{xz},d_{yz}) and b_{2g} (d_{xy}) orbitals. The fully occupied heavily 4s/dz^2 mixed ligand bonding a_{1g} MO is traditionally (based on CFT) placed between the a_{1g} and e_g, b_{2g} MO energy levels, however in real systems (with ligand MOs included) it is typical for the energy of this *bonding* MO to drop below the *non-bonding* e_g, b_{2g} MO energy levels.

The pseudo- symmetry of $[Cu(acac)(tmen)]^+$ is C_{2v}, below that of D_{4h}, this drop in symmetry allows further interaction between the ligand and metal fragment orbitals, and additional mixing interactions between the resultant MOs. A change in the principle axis orientation between the ideal ML_4 D_{4h} and more representative $ML_2L'_2$ C_{2v} complex makes formal assignment of the dAO contributions to the real MOs a complex procedure. To expedite interpretation, symmetry labels will be given but these are only approximate and relate back to the original CFT labels that the majority of readers are most familiar with.

A detailed MO analysis was carried out for the $[Cu(acac)(tmen)]^+$ cation in the gas phase. Both unrestricted and restricted open shell calculations was carried out on a fully optimised (open shell) structure using the B3LYP functional in conjunction with an aug-cc-pVTZ basis set for the first row heavy atoms and a cc-pVTZ basis set for the H-atoms. The Cu-atom was modelled using a scalar relativistic Stuttgart PP (ECP10MWB) and the associated basis set.[11]

To aid in interpretation the MOs presented in **Figure 5** are from a restricted open shell calculation where paired electrons (alpha and beta spin) are forced to occupy the same spatial orbital (these are the standard MOs normally depicted). In a system with unpaired spins, the exchange between all orbitals of the same spin means that the spatial orbitals of the alpha and beta spin electrons differ (as there is one more alpha than beta spin electron) the spatially relaxed orbitals for each spin have been examined and most do not differ substantially from the unrestricted (U) orbitals. The one exception is the partially occupied alpha dx^2-y^2 MO which is lower in energy than the alpha ligand orbital, leading the ligand alpha orbital to become the system and alpha HOMO for the unrestricted system, the beta HOMO is still the ligand orbital.

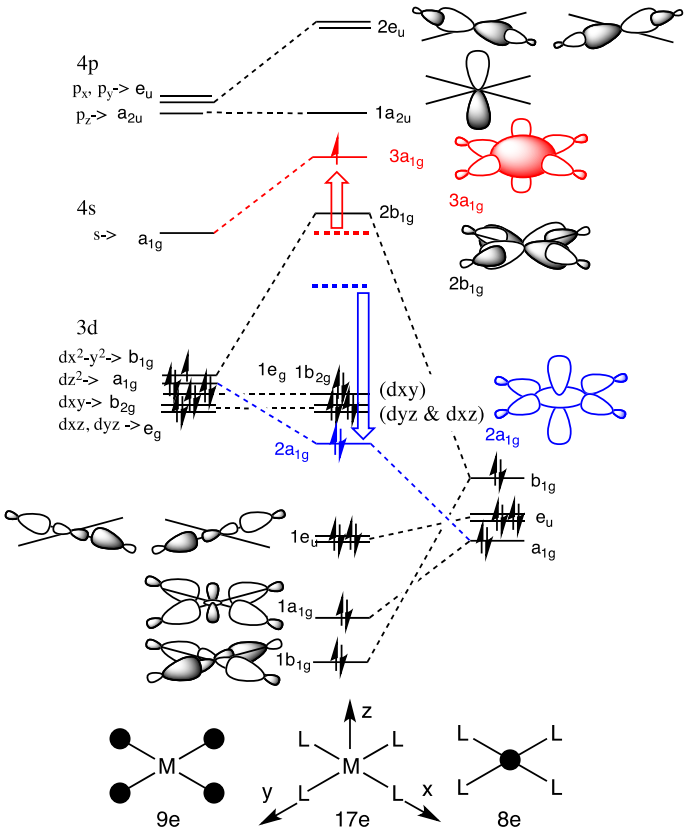

Figure S4.1.1: Tetragonal distortion from octahedral to produce a square planar complex.

4.2 TD-DFT calculations and UV-Vis Spectral analysis

For each functional (B3lYP, M06, M06-L and M06-HF) a TD-DFT calculation of the 25 lowest excited states (multiplicity 2, unrestricted spin) was carried out to determine the UV-Vis spectra in the gas and solution phase. TD-DFT calculations determine an excitation wavelength, an *oscillator strength* (*f*) and the *Frank-Condon factor*. The oscillator strength is a dimensionless quantity normally between 0.1-1.0 dependent on the square of the (electronic) transition dipole moment (the dipole moment of light connecting the initial and final states of the molecule). The overlap integral $S(\nu,\nu')$ represents the sum of the overlap of the ground and excited vibrational states, this allows formally forbidden transitions via vibronic coupling. The total oscillator strength is a product of the electronic oscillator strength (f) and the Frank-Condon factor (S).

Figure S4.2.1a compares the functionals including various amounts of exchange. **Figure S4.2.1b** compares the gas-phase and IL environment for selected functionals. The oscillator strength and Frank-Condon factor for the 14 lowest excitations of the $[Cu(acac)(tmen)]^+$ cation are reported for the gas phase (**Table S4.2.1**) and for the cation within an IL-SMD environment (**Table S4.2.2**). The primary excitations associated with the transitions with greatest oscillator strength are highlighted in bold in **Tables S4.2.1-2** and are detailed more fully in **Table S4.2.3**, the relevant MOs; the HOMO-3, HOMO and LUMO are depicted in **Figure S4.2.2**.

Principle transitions were identified as those with a large Frank-Condon factor, in the B3LYP calculation the most significant transition is from a nominal dz^2 type MO to the dx^2-y^2 type MO (255nm), this transition showed mixed character and only the dominant contribution is identified here (0.52). Two other transitions had appreciable Frank-Condon factors, both have a clearly resolved character; one is a lower energy ligand to metal charge transfer (339nm) and the other is a

higher energy ligand to ligand excitation (243nm). These transitions are all identified in **Figure 4** of the paper.

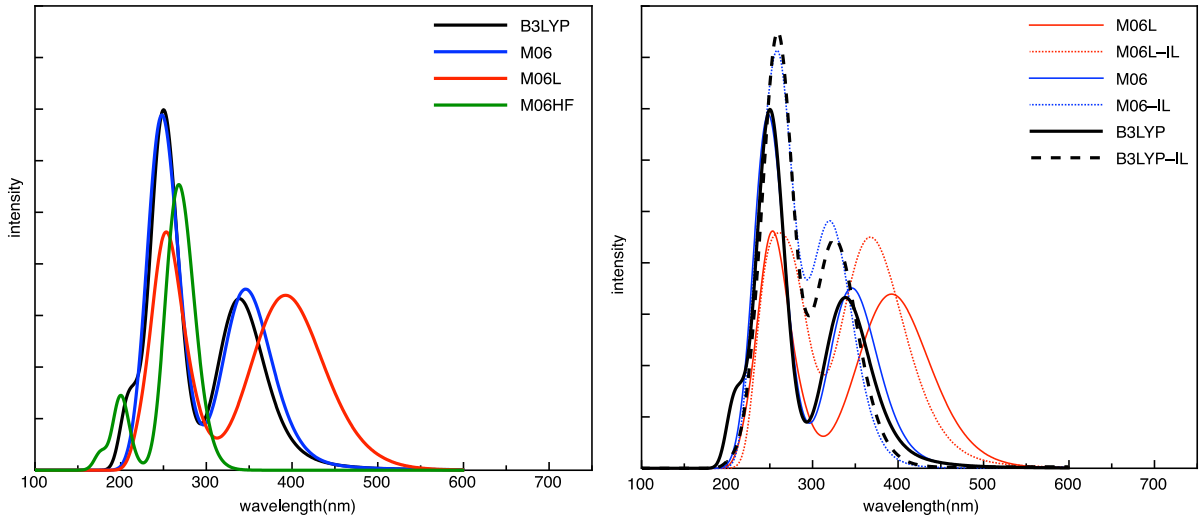

Figure S4.2.1: computed UV-Vis spectra for $[Cu(acac)(tmen)]^+$ (a) comparing B3LYP and a range of M06 functionals in the gas-phase, (b) comparing spectra computed in the gas-phase (GP) and a generalized solvent environment of $[C_4C_1im][PF_6]$ (IL)

Table S4.2.1. Gas phase TD-DFT, oscillator strength (*f*), and orbital transition analysis for selected transitions. B3LYP, M06 & M06L

State	gas-phase (M06L) λ (nm)	*f*	gas-phase (B3LYP) λ (nm)	*f*	gas-phase (M06) λ (nm)	*f*
exchange	0%		20%		27%	
S1	680	0.000	568	0.000	625	0.000
S2	462	0.000	506	0.000	621	0.000
S3	420	0.004	474	0.001	539	0.001
S4	405	0.000	464	0.000	518	0.000
S5	**404**	**0.119**	405	0.007	435	0.003
S6	380	0.000	394	0.000	374	0.000
S7	373	0.000	**338**	**0.162**	**346**	**0.170**
S8	**372**	**0.053**	321	0.000	312	0.006
S9	344	0.025	304	0.003	310	0.002
S10	282	0.037	260	0.011	**261**	**0.122**
S11	268	0.025	**255**	**0.194**	252	0.022
S12	265	0.007	251	0.024	249	0.034
S13	256	0.000	**243**	**0.141**	**247**	**0.122**
S14	254	0.003	235	0.000	**239**	**0.092**
S15	**254**	**0.150**	225	0.004	237	0.000

Table S4.2.2. IL-TD-DFT Calculated energy levels, oscillator strength (*f*), and orbital transition analysis for selected transitions. B3LYP, M06 & M06L

State	IL (M06L) λ (nm)	*f*	IL (B3LYP) λ (nm)	*f*	IL (M06) λ (nm)	
exchange	0%		20%		27%	
S1	555	0.000	592	0.001	665	0.000
S2	504	0.002	563	0.000	621	0.001
S3	433	0.001	516	0.000	611	0.000
S4	430	0.000	511	0.000	565	0.000
S5	413	0.000	392	0.000	384	0.002
S6	389	0.049	385	0.002	369	0.000
S7	379	0.000	335	00002	333	0.000
S8	**367**	**0.169**	**326**	**0.217**	**321**	**0.228**
S9	334	0.041	297	0.004	298	0.010
S10	297	0.002	270	0.005	263	0.003
S11	**283**	**0.089**	**262**	**0.358**	**263**	**0.326**
S12	278	0.019	255	0.017	257	0.014
S13	274	0.034	242	0.000	251	0.001
S14	267	0.030	241	0.083	249	0.001

Table S4.2.3: Primary excitations for the gas phase structures

State	M06L λ (nm) *f*	*excitations*	State	B3LYP λ (nm) *f*	*excitations*	State	M06 λ (nm) *f*	*excitations*
S1	680 0.000	**73B→74B** **L→dx²-y²**	S1	568 0.000	57B→69B 58B→69B 62B→69B **68B→69B** **L→dx²-y²**	S1	625 0.000	57B→74B 60B→74B 67B→74B **73B→74B**
S5	404 0.119	68B→74B **72B→74B** **L→dx²-y²**	S7	338 0.162	57B→69B 62B→69B **67B→69B** **L→dx²-y²**	S7	404 0.170	60B→74B 67B→74B **72B→74B**
S15	254 0.150	72A→75A 73A→75A 74A→76A **73B→75B** **L→L***	S11	255 0.194	69A→70A 56B→69B 61B→69B **65B→70B** **dz²→dx²-y²**	S10	261 0.122	73A→75A 62B→74B 64B→74B **70B→74B** 73B→75B

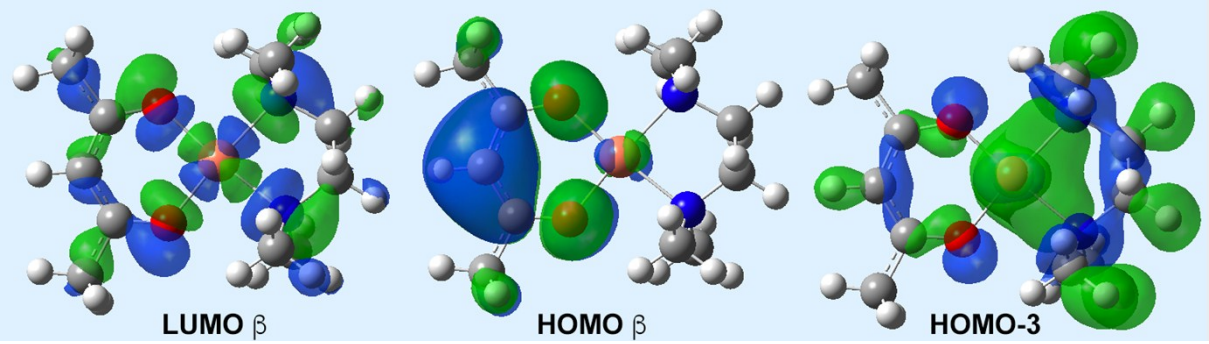

Figure S4.2.2: key B3LYP orbitals for the transitions

The allowed transitions all occur in the UV-region of the spectrum and are not observable using standard UV-Vis spectrometers. d-d transitions such as those giving rise to the observed colour of these solutions are formally forbidden. We have examined the contributing MOs and evaluated those transitions which can contribute to d-d transitions focusing on those of the lowest energy and likely, through vibronic coupling, to give rise to the observed transitions in the visible region.

The dx^2-y^2 MO is the HOMO for alpha electrons and LUMO for beta electrons, **Figure S4.2.2a**. The beta HOMO (**Figure S4.2.2b**) through to HOMO-2 are ligand Lπ* MOs, lying below these are the d-AO manifold of MOs, the HOMO-3 is the highest energy in the d-AO manifold and is a dz^2 based MO. Note that all of traditionally assigned "d-AOs" contain significant ligand contributions. The relative ordering of these orbitals can differ slightly depending on the functional (amount of exchange) and the environment, however the overall shape and LCAOs of these MOs remains consistent.

The lowest energy excitation (S1) is formally forbidden and is a HOMO to LUMO transition from a ligand Lπ* MO -> dx^2-y^2 MO. The first key transition from a dz^2 based MO to the dx^2-y^2 LUMO for the gas-phase, and in the non-interacting IL $[C_4C_1im][PF_6]$, are detailed in **Table S4.2.4**, this is generally,

but not always, the second excitation (S2). The experimental wavelength of the peak maxima for the $[Cu(acac)(tmen)]^+$ cation in $[C_4C_1im][PF_6]$ is at λ=514nm, thus the computed wavelength for the gas-phase B3LYP calculation coincides best with the experimental data λ=506nm.

Table S4.2.3: wavelength of key transitions from the occupied dz^2 based MO to the dx^2-y^2 LUMO for the gas phase and in $[C_4C_1im][PF_6]$ for the M06L, B3LYP and M06 functionals. The order of the excitation is given in brackets.

$dz^2 \rightarrow dx^2$-y^2	λ (nm) gas-phase	λ (nm) $[C_4C_1im][PF_6]$	λ (nm) shift in IL
M06L (0%)	462 (S2)	504 (S2)	+42
B3LYP (20%)	506 (S2)	592 (S1)	+86
M06 (27%)	539 (S3)	621 (S2)	+82

Section 5: Counter anion-association

Table 5.1. Relative permittivity ε[12] and Kamlet-Taft β values for the ILs discussed in the paper.

Solution	ε (25 °C)	Kamlet-Taft β value
$[C_4C_1im]Cl$	-	0.87[13]/0.95[14]
$[C_4C_1im][SCN]$	13.7±0.8	0.71[14]
$[C_4C_1im][NO_3]$	-	0.74[14]
$[C_4C_1im][OTf]$	12.9±0.5	0.46[15]/0.49[16]/0.53[14]
$[(OH)^3C_3C_1im][NTf_2]$	-	0.29[17]
$[(CN)^3C_3C_1im][NTf_2]$	-	0.22[18]
$[C_2C_1im][ClO_4]$*	-	0.41[19]
$[C_4C_1im][NTf_2]$	14.0±0.5	0.24[15,20]/0.42[14]
$[C_4C_1C_1im][NTf_2]$	14.0±0.8	0.24[15]
$[C_4C_1pyrr][NTf_2]$	15.3±0.5	0.25[15]/0.24[20]
$[C_4C_1im][PF_6]$	14.0±0.7	0.21[15,16]/0.44[14]

***** Bearing in mind that Kamlet-Taft β value is mainly affected by the anion[19], the data for $[ClO_4]^-$ anion combined with $[C_2C_1im][ClO_4]$ was used as the only literature available.

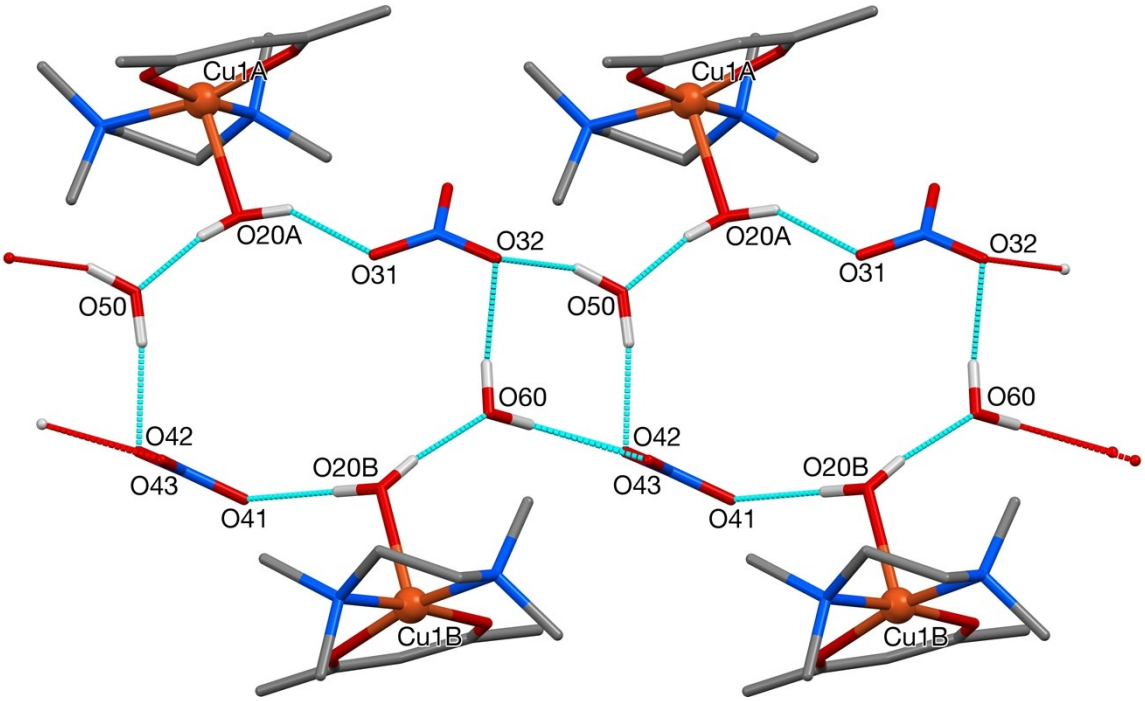

Figure 5.1. The crystal structure of [Cu(acac)(tmen)(H_2O)][NO_3] showing part of the ribbon along the crystallographic *a* axis direction formed by the two independent cations, anions and included water molecules

Section 6.0: Determination of ILs DN

Table S6.1. Absorption maxima vs DN for $[Cu(acac)(tmen)]^+$ complexes in various solvents.

$\varepsilon_{max} \approx 10^2 dm^3 mol^{-1} cm^{-1}$ for all absorptions.

Solvent	Gutmann Donor Number DN	νmax /10^3 cm^{-1}				
		[Cu acac tmen]$^+$ anion				
		$[NO_3]^-$	$[PF_6]^-$	$[OTf]^-$	$[NTf_2]^-$	$[SCN]^-$
pyridine	33.1	15.6	15.6	15.6	15.6	14.4
DMSO	29.8	16.3	16.3	16.3	16.3	16.0
DMF	26.6	16.5	16.5	16.5	16.5	15.8
methanol	19.1	17.0	17.0	17.0	17.0	16.8
1,4-dioxane	14.8	17.0	17.0	17.0	17.0	14.4
acetonitrile	14.1	17.3	17.3	17.3	17.3	15.7
benzonitrile	11.9	17.3	17.8	17.4	17.8	14.8
nitromethane	2.7	18.5	19.0	18.9	19.0	15.5
$[C_4C_1im][NO_3]$	-	16.3	-	-	-	-
$[C_4C_1im][PF_6]$	-	-	19.4	-	-	-
$[C_4C_1C_1im][PF_6]$	-	-	19.1	-	-	-
$[C_4C_1im][OTf]$	-	-	-	17.2	-	-
$[C_4C_1im][NTf_2]$	-	-	-	-	18.2	-
$[C_4C_1im][SCN]$	-	-	-	-	-	14.3

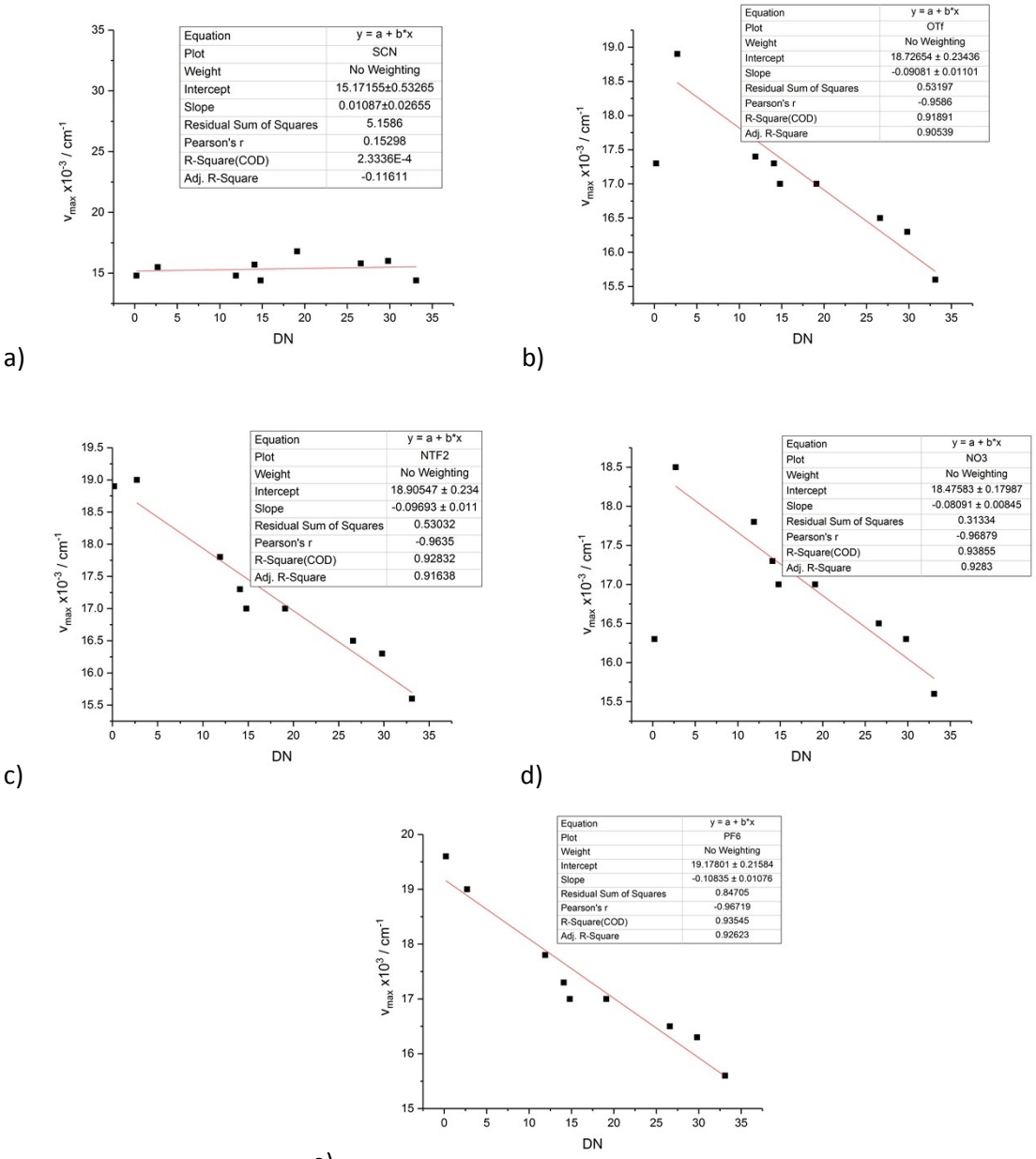

Figure S6.1. Linear plots of absorption maxima vs DN of $[Cu(acac)(tmen)]^+$ complexes with different anions: a)$[SCN]^-$;b) $[OTf]^-$; c)$[NTf_2]^-$; d)$[NO_3]^-$; e)$[PF_6]^-$.

Section 7: Computed partial charges for model probe cations

a. (Acetylacetonato)(*N*,*N*,*N*'*N*'-tetramethylethylenediamine)copper(II): $[Cu(acac)(tmen)]^+$

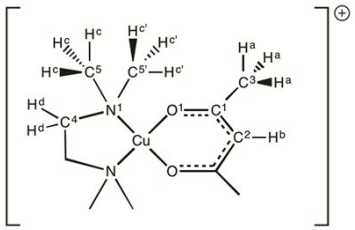

Figure S7.1. Atom labelling for the $[Cu(acac)(tmen)]^+$ cation.

Table S7.1. Computed partial charges (e) for the $[Cu(acac)(tmen)]^+$ cation. Σ(acac) corresponds to the total sum of the individual partial charges for all atoms in a single acac ligand, Σ(tmen) corresponds to the total sum of atomic partial across the tmen ligand.

	M06/aug-cc-pVDZ		**M06-L/aug-cc-pVDZ**	
	NBO	**CHELPG**	**NBO**	**CHELPG**
Cu	**0.917**	**0.546**	**1.040**	**0.546**
O1	-0.350	-0.554	-0.733	-0.554
C1	0.279	0.705	0.536	0.705
C2	-0.252	-0.692	-0.469	-0.692
C3	-0.345	-0.397	-0.676	-0.397
Ha (average)	0.127	0.130	0.246	0.130
Hb	0.127	0.171	0.246	0.171
Σ(acac)	**-0.471**	**-0.083**	**-0.491**	**-0.083**
N1	-0.260	-0.056	-0.585	-0.056
C4	-0.122	-0.025	-0.222	-0.025
C5	-0.221	-0.209	-0.402	-0.209
C5’	-0.216	-0.185	-0.410	-0.185
Hc (average)	0.119	0.114	0.229	0.114
Hc’ (average)	0.119	0.107	0.228	0.107
Hd (average)	0.123	0.076	0.236	0.076
Σ(tmen)	**0.554**	**0.537**	**0.394**	**0.537**

b. Copper (II) acetylacetonate: $Cu(acac)_2$

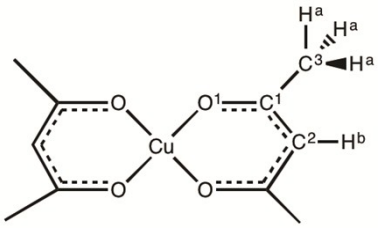

Figure S7.2. Atom labelling for the $Cu(acac)_2$ complex.

Table S7.2. Computed partial charges (e) for the neutral $Cu(acac)_2$ complex. Σ(acac) corresponds to the total sum of the individual partial charges for all atoms in a single acac ligand.

	M06/aug-cc-pVDZ		M06-L/aug-cc-pVDZ	
	NBO	**CHELPG**	**NBO**	**CHELPG**
Cu	**1.387**	**0.811**	**1.341**	**0.761**
O1	-0.775	-0.575	-0.742	-0.540
C1	0.552	0.751	0.519	0.724
C2	-0.537	-0.815	-0.500	-0.789
C3	-0.700	-0.384	-0.679	-0.399
Ha (average)	0.242	0.108	0.235	0.110
Hb	0.235	0.180	0.226	0.179
Σ(acac)	**-0.693**	**-0.406**	**-0.671**	**-0.381**

c. Copper (II) hexafluoroacetylacetonate: $Cu(hfac)_2$

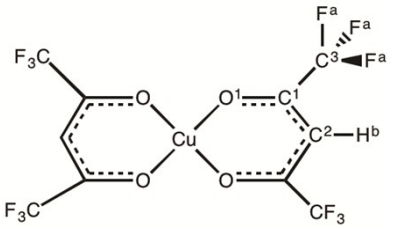

Figure S7.3 Atom labelling for the $Cu(hfac)_2$ complex.

Table S7.3. Computed partial charges (e) for the neutral $Cu(hfac)_2$ complex. Σ(hfac) corresponds to the total sum of the individual partial charges for all atoms in a single hfac ligand.

	M06/aug-cc-pVDZ		M06-L/aug-cc-pVDZ	
	NBO	**CHELPG**	**NBO**	**CHELPG**
Cu	**1.402**	**0.895**	**1.357**	**0.850**
O1	-0.726	-0.506	-0.695	-0.476
C1	0.467	0.512	0.434	0.502
C2	-0.507	-0.563	-0.473	-0.560
C3	1.145	0.530	1.123	0.470
Fa (average)	-0.375	-0.186	-0.367	-0.170
Hb	0.284	0.158	0.274	0.160
Σ(hfac)	**-0.701**	**-0.447**	**-0.679**	**-0.425**

d. Copper (II) dithioacetylacetonate: $Cu(sacsac)_2$

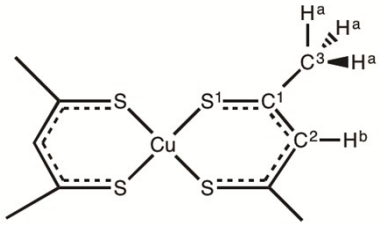

Figure S7.4. Atom labelling for the $Cu(sacsac)_2$ complex.

Table S7.4. Computed partial charges (e) for the neutral $Cu(sacsac)_2$ complex. Σ(sacsac) corresponds to the total sum of the individual partial charges for all atoms in a single sacsac ligand.

	M06/aug-cc-pVDZ		M06-L/aug-cc-pVDZ	
	NBO	**CHELPG**	**NBO**	**CHELPG**
Cu	**0.828**	**0.301**	**0.871**	**0.363**
S1	-0.139	-0.270	-0.142	-0.290
C1	-0.061	0.267	-0.080	0.284
C2	-0.377	-0.319	-0.345	-0.348
C3	-0.675	-0.148	-0.653	-0.152
Ha (average)	0.247	0.062	0.239	0.061
Hb	0.233	0.102	0.224	0.118
Σ(sacsac)	**-0.414**	**-0.150**	**-0.435**	**-0.182**

d. Comparison of partial charges on copper centres

Table S7.5. Comparison of the computed partial charges (*e*) on the copper centres across the selected copper complexes.

	M06/aug-cc-pVDZ		M06-L/aug-cc-pVDZ	
Copper complex	**NBO**	**CHELPG**	**NBO**	**CHELPG**
$Cu(sacsac)_2$	0.83	0.30	0.87	0.36
[Cu(acac)(tmen)]+	0.92	0.55	1.04	0.55
$Cu(acac)_2$	1.39	0.81	1.34	0.76
$Cu(hfac)_2$	1.40	0.89	1.36	0.85

Small changes in geometry between the M06 and M06-L structures do not significantly alter the partial charges on the Cu centres.

For a given copper complex, the NBO and CHELPG methods produce notably different charges; the magnitude of the NBO partial charge on Cu is greater in each case. Discrepancies between the two schemes have been noted elsewhere. However, both the NBO and CHELPG schemes predict the same *ordering* for the Cu partial charges across the four complexes:

$$Cu(hfac)_2 > Cu(acac)_2 > [Cu(acac)(tmen)]^+ > Cu(sacsac)_2$$

Using the NBO and CHELPG partial charges in **Table S7.5**, two neutral complexes, $Cu(hfac)_2$ and $Cu(acac)_2$, are predicted to have larger positive charges on the Cu centre than found within cationic $[Cu(acac)(tmen)]^+$. This result emphasises the importance of considering the local environment of the Cu centre. Replacing the highly electronegative oxygen atoms of the acac ligands with sulphur, to form $Cu(sacsac)_2$, is predicted to lead to a reduction in the positive charge on the Cu centre relative to $[Cu(acac)(tmen)]^+$.

Section 8: Application of $Cu(sacsac)_2$ for DN determination

$[Cu(sacsac)_2]$ shows a complex absorption spectrum, similar to the previously reported $[Cu(acac)_2]$.[21] The spectra were deconvoluted using a non-linear Gaussian fit. Fits were attempted for combinations of 3, 4 and 5 peaks. A best fit was obtained for four peaks (see **Figure S8.1**). The absorption maxima (ν1-ν4) for all four fitted peaks, in a range of molecular solvents and ILs, were obtained (**Table S8.1**). These were plotted versus the DN numbers of the corresponding molecular solvents, **Figure S8.2**. Linear fits were obtained and compared, only peaks ν2 and ν4 were observed for all molecular solvents, as a very shallow slope of ν4 makes the calculation of DN unreliable, the linear fit from the peak 2 (ν2) in the region 20.7-22.4 ($*10^3$) cm^{-1} was chosen and employed in the calculation of DNs for the ILs.

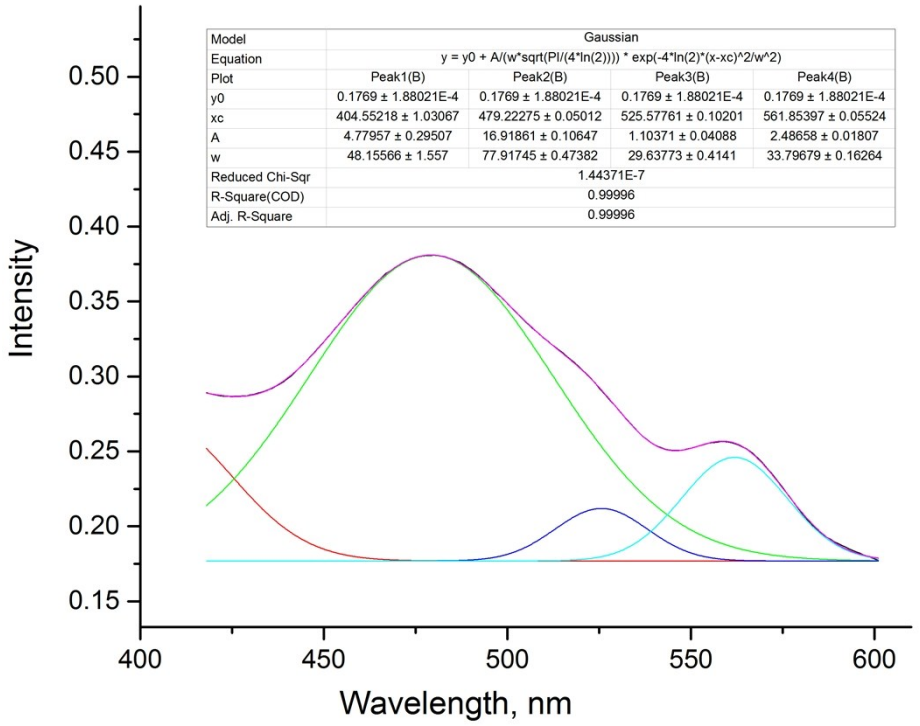

Fuigure S8.1. Example showing the deconvoluted spectrum of the $Cu(sacsac)_2$ complex in methanol.

Table S8.1. The absorption maxima (ν_{max}) of the $Cu(sacsac)_2$ complex in a range of molecular solvents and ILs.

Molecular solvent	DN	Deconvoluted peaks ν_{max}, cm^{-1}			
		1	2	3	4
DMSO	29.8	-	20.7	18.1	16.5
Methanol	19.1	24.7	20.9	19.0	17.8
Acetonitrile	14.1	22.6	21.3	19.4	-
Chloroform	4	-	22.4	18.8	17.6
DCE	0	22.3	21.0	18.7	17.7
$[C_4C_1im][PF_6]$		24.4	20.7	19.0	17.8
$[C_4C_1im][OTf]$		24.1	20.8	19.1	17.2
$[C_4C_1im][NTf_2]$		25.4	22.5	18.9	17.7
$[C_4C_1C_1im][NTf_2]$		-	20.9	18.9	17.7
$[(HO)^3C_3C_1im][NTf_2]$		24.0	21.4	19.2	17.8
$[C_4C_1im][SCN]$		-	20.6	19.2	17.4

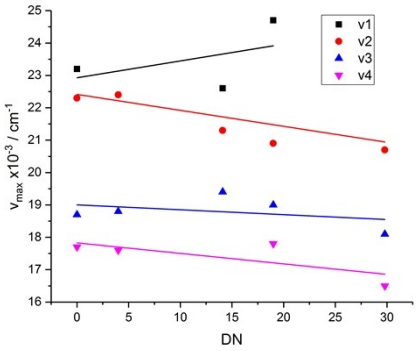

Figure S8.2 Plot of linear fit for DN determination with $Cu(sacsac)_2$ complex

Table S8.2. Least squares fit to the peak maxima data.

Equation	y = a + b*x	y = a + b*x	y = a + b*x	y = a + b*x
Plot	ν1	ν2	ν3	ν4
Intercept	22.93 ± 1.32	22.41 ± 0.51	19.00 ± 0.36	17.83 ± 0.37
Slope	0.05 ± 0.1	-0.05 ± 0.03	-0.02 ± 0.02	-0.03 ± 0.02
R-Square(COD)	0.22445	0.42519	0.14449	0.54297
Adj. R-Square	-0.55109	0.28149	-0.14067	0.31446

References

1 V. Polshettiwar and M. P. Kaushik, *Tetrahedron Lett.*, 2004, **45**, 6255.

2 M. J. Frisch, G. W. Trucks, H. B. Schlegel, G. E. Scuseria, M. A. Robb, G. Cheeseman, J. R.; Scalmani, V. Barone, B. Mennucci, G. A. Petersson, H. Nakatsuji, M. Caricato, X. Li, H. P. Hratchian, A. F. Izmaylov, J. Bloino, G. Zheng, J. L. Sonnenberg, M. Hada, M. Ehara, K. Toyota, R. Fukuda, J. Hasegawa, M. Ishida, T. Nakajima, Y. Honda, O. Kitao, H. Nakai, T. Vreven, J. Montgomery, J. A., J. E. Peralta, F. Ogliaro, M. Bearpark, J. J. Heyd, E. Brothers, K. N. Kudin, V. N. Staroverov, R. Kobayashi, J. Normand, K. Raghavachari, A. Rendell, J. C. Burant, S. S. Iyengar, J. Tomasi, M. Cossi, N. Rega, J. M. Millam, M. Klene, J. E. Knox, J. B. Cross, V. Bakken, C. Adamo, J. Jaramillo, R. Gomperts, R. E. Stratmann, O. Yazyev, A. J. Austin, R. Cammi, C. Pomelli, J. W. Ochterski, R. L. Martin, K. Morokuma, V. G. Zakrzewski, G. A. Voth, P. Salvador, J. J. Dannenberg, S. Dapprich, A. D. Daniels, Ö. Farkas, J. B. Foresman, J. V. Ortiz, J. Cioslowski and D. J. Fox, 2009.

3 Y. Zhao and D. G. Truhlar, *Theor. Chem. Acc.*, 2008, **120**, 215.

4 C. M. Breneman and K. B. Wiberg, *J. Comput. Chem.*, 1990, **11**, 361.

5 E. Sigfridsson, U. L. F. Ryde, T. Chemistry, C. Centre and P. O. Box, *J. Comput. Chem.*, 1998, **19**, 377.

6 E. D. Glendening, J. K. Badenhoop, A. E. Reed, J. E. Carpenter, J. A. Bohmann, C. M. Morales

and F. Weinhold, 2009.

7 Y. Zhao and D. G. Truhlap, *Acc. Chem. Res.*, 2008, **41**, 157.

8 D. Jacquemin, E. A. Perpète, I. Ciofini, C. Adamo, R. Valero, Y. Zhao and D. G. Truhlar, *J. Chem. Theory Comput.*, 2010, **6**, 2071.

9 Y. Zhao and D. G. Truhlar, *J. Chem. Phys.*, 2006, **125**, 194101.

10 V. S. Bernales, A. V. Marenich, R. Contreras, C. J. Cramer and D. G. Truhlar, *J. Phys. Chem. B*, 2012, **116**, 9122.

11 M. Dolg, U. Wedig, H. Stoll and H. Preuss, *J. Chem. Phys.*, 1987, **86**, 417.

12 M. M. Huang, Y. Jiang, P. Sasisanker, G. W. Driver and H. Weingärtner, *J. Chem. Eng. Data*, 2011, **56**, 1494.

13 H. Ohno and Y. Fukaya, *Chem. Lett.*, 2009, **38**, 2.

14 R. Lungwitz, M. Friedrich, W. Linert and S. Spange, *New J. Chem.*, 2008, **32**, 1493.

15 L. Crowhurst, P. R. Mawdsley, J. M. Perez-Arlandis, P. A. Salter and T. Welton, *Phys. Chem. Chem. Phys.*, 2003, **5**, 2790.

16 M. A. A. Rani, A. Brant, L. Crowhurst, A. Dolan, M. Lui, N. H. Hassan and J. P, *Phys. Chem. Chem. Phys.*, 2011, **13**, 16831.

17 Y. Wu, T. Sasaki, K. Kazushi, T. Seo and K. Sakurai, *J. Phys. Chem. B*, 2008, **112**, 7530.

18 C. Chiappe, D. Pieraccini, D. Zhao, Z. Fei and P. J. Dyson, *Adv. Synth. Catal.*, 2006, **348**, 68.

19 S. Zhang, X. Qi, X. Ma, L. Lu and Y. Deng, *J. Phys. Chem. B*, 2010, **114**, 3912.

20 S. Coleman, R. Byrne, S. Minkovska and D. Diamond, *Phys. Chem. Chem. Phys.*, 2009, **11**, 5608.

21 R. L. Belford, M. Calvin and G. Belford, 1957, **26**, 1165.